RSC Advances

PAPER

View Article Online
View Journal | View Issue

Cite this: *RSC Adv.*, 2022, **12**, 19990

Using starch graft copolymer gel to assist the CO_2 huff-n-puff process for enhanced oil recovery in a water channeling reservoir

Hongda Hao, *[a] Dengyu Yuan,[b] Jirui Hou,[c] Wenmin Guo[a] and Huaizhu Liu[d]

The CO_2 huff-n-puff process is an effective method to enhance oil recovery (EOR) and reduce CO_2 emissions. However, its utilization is limited in a channeling reservoir due to early water and gas breakthrough. A novel starch graft copolymer (SGC) gel is proposed for treating the channels and assisting with the CO_2 huff-n-puff process. Firstly, the bulk and dynamic performances of the SGC gel including rheology, injectivity and plugging ability are compared with the polymer gel in the laboratory. Then, 3D physical models with water channels are established to reveal the EOR mechanisms of gel assisted CO_2 huff-n-puff. Several pilot tests of gel assisted CO_2 huff-n-puff are also discussed in this paper. The bulk and dynamic experimental results show that although these two gelants have similar viscosities, the SGC gelant has a better injectivity compared with the polymer gelant. The SGC gel is predominantly a viscous solution, which make it easier to flow through the pore throats. The RF of the SGC gelant is only 0.58 times that of the polymer gelant. After the gelation, a 3D network-like gel with a viscosity of 174 267 mPa s can be formed using the SGC gelant. The RRF of the SGC gel is about three times that of the polymer gel, which shows that the SGC gel has a stronger plugging ability within the porous media. The 3D experimental results show that four cycles of gel assisted CO_2 huff-n-puff can achieve an EOR of 11.36%, which is 2.56 times that of the pure CO_2 huff-n-puff. After the channels are plugged by the SGC gel, the remaining oil of the near-wellbore area can be first extracted by CO_2, and the oil of the deep formation can then be effectively displaced by the edge water. Pilot tests on five wells were conducted in the Jidong Oilfield, China, and a total oil production of 3790.86 m^3 was obtained between 2016 and 2021. The proposed novel SGC gel is suitable for assisting with the CO_2 huff-n-puff process, which is a beneficial method for further EOR in a water channeling reservoir.

Received 20th March 2022
Accepted 26th June 2022

DOI: 10.1039/d2ra01812h

rsc.li/rsc-advances

1. Introduction

With the growing consumption of energy in the world, the development of heavy oil reserves becomes increasingly important for the petroleum industry. A number of heavy oil reservoirs located in China have edge or bottom water.[1–3] On one hand, the edge or bottom water could provide energy for the oil production, on the other hand, the invasion of water could also cause a quick increase of water cut.[4,5] The North Gaoqian Block, Jidong Oil Field, China has been developed using horizontal wells since 2004, however, the water cut increased sharply from 86% to 99% after five years of development. This is because of: (1) a large viscosity contrast between the water and oil decreases the flooding efficiency of edge water, and (2) large pore throats gradually form water channels, which then causes a bypass of the formation of oil. Enhanced oil recovery (EOR) from these reservoirs with serious water channeling has become one of the biggest challenges in oilfield development.

The CO_2 huff-n-puff has been proved to be an effective method for enhanced heavy oil recovery. The oil recovered by CO_2 is mainly due to viscosity reduction, oil swelling, light components of oil extraction, and relative permeability of water and gas reduction.[6–10] The North Gaoqian Block has also used CO_2 huff-n-puff since 2010, and about 16×10^4 t of heavy oil was recovered by the end of 2017. However, the oil recovery gradually decreased after multiple cycles of huff-n-puff, especially for those wells located in water channeling zones, and the oil recovery decreased sharply after one or two cycles of huff-n-puff. The water channels not only provide pathways for the invaded edge water, but also lower the EOR efficiency of the CO_2 injection.[11,12] Thus, treatments need to be implemented to assist CO_2 huff-n-puff in these water channeling zones.

[a]*School of Petroleum Engineering, Changzhou University, Changzhou, Jiangsu, 213164, China. E-mail: haohongda90@126.com; Tel: +86 17601007653*

[b]*Exploration and Development Research Institute, PetroChina Daqing Oilfield Company, Daqing, Heilongjiang 163000, China*

[c]*Research Institute of Unconventional Oil & Gas Science and Technology, China University of Petroleum, Beijing 102249, China*

[d]*Drilling and Production Technology Research Institute, PetroChina Jidong Oilfield Company, Tangshan, Hebei 063000, China*

Various chemical methods are proposed for EOR including low salinity waterflooding (LSW), polymer flooding, nanoparticle (NP) flooding, and so on. The LSW is considered as a newly developed EOR method in both sandstone and carbonate reservoirs. After injecting brine of a low salinity into the oil reservoir, oil/brine/rock interactions could be affected in a favorable manner to reduce the remaining oil saturation, however, few successful applications of LSW are reported in field tests.[13–15] Polymer flooding is the most applied EOR technique with the assistance of viscous fingering reduction, permeability reduction and the viscoelastic behavior of the polymer, and researchers have shown that about 5% of tertiary oil recovery can be obtained using polymer flooding. However, problems such as low tolerance of temperature, poor salinity resistance and high susceptibility to oxidative degradation may limit the utilization of the polymer. Then, alkaline polymer (AP), micellar polymer (MP), alkaline surfactant polymer (ASP) and even nanoparticles (NPs) are successively proposed for further enhanced oil recovery.[16,17] In recent years, NPs have provided great potential for the EOR process with the rapid evolution of nanotechnology, and various types of NPs have been studied both in the laboratory and in field tests. Wettability alteration, interfacial tension (IFT) reduction, emulsification and solubilization are usually associated with the NPs, however, further EOR mechanisms still need to be clearly determined during NP flooding.[18–21]

For further EOR during the CO_2 injection process, water alternating-gas (WAG) is commonly used because water injection is helpful for improving the macroscopic sweep efficiency, and the water/gas slug ratio needs to be carefully designed to obtain a favorable oil recovery.[22,23] Nitrogen (N_2) is also used to assist with CO_2 injection due to its strong ability of pressure maintenance, however, its applications are limited in coal bed methane or pressure depleted oil reservoirs.[24,25] Foaming agents are reported to be helpful reagents to control water and gas mobilities in heterogeneous reservoirs, which can be used to assist with the CO_2-EOR process, however, its application is still limited under serious channeling conditions due to the weak stability of the foam.[26–28] Because gel usually has a higher blocking strength compared to foam, it is more suitable to treat large-scale channels. The *in situ* polymer-based gels including partially hydrolyzed polyacrylamide (HPAM) gel are the most widely used for water management in oil reservoirs. When the gelant is injected into the formation, *in situ* inter-molecule crosslinking reactions will occur between the HPAM, crosslinker and other reagents, which then form a strong barrier for water plugging. Since Sydansk[29] first proposed that a HPAM/Cr(III) gel had a potential application in oilfields, researchers have developed various types of polymer gels. For example, Sengupta *et al.*[30] used hydroquinone (HQ) and hexamethylenetetramine (HMTA) to form a polymer gel, which could be maintained at a high strength under 120 °C. Zhao *et al.*[31] prepared a polyacrylamide (PAM) gel with the addition of phenolic resin and nonionic PAM, which had a satisfactory gelation time and a high strength for plugging. In order to improve the plugging performance, SiO_2 was added with the polymer to enhance the structural strength of the gel.[32,33] However, when applying the polymer gel treatment, its plugging performance would also be negatively affected by the acidic environment created by the CO_2 injection, chromatographic separation of the chemical reagents and irreversible formation damage caused by the polymer injection.[34,35] Therefore, it is necessary to find a novel gel with stable properties to assist with the CO_2 huff-n-puff.

Bal *et al.*[36] created a foam–gel formulation with hydrolyzed PAM crosslinked by chromium triacetate in the presence of alpha-olefin sulfonate. The foam gel layer could withstand a CO_2 pressure gradient of 0.7 kg cm^{-2} over a length of 30.48 cm without rupture, and could be used as a sealant for plugging reservoir fractures. Zhang *et al.*[37] proposed a DOAPA/SPTS system by mixing 4.4 wt% *N*,*N*-dimethyl octylamide-propyl tertiary amine (DOAPA) and 2.0 wt% sodium *p*-toluenesulfonate (SPTS). This system forms wormlike micelles (WLMs) which can generate a bulk gel, which is expected to mitigate CO_2 channeling in ultra-low permeability reservoirs. Zhou *et al.*[38] used cyclodextrin to create an inclusion polymer gel. The cyclodextrin in the gel can reorganize an amphiphilic polymer which has been broken *via* a host–guest inclusion effect, so it has a better shear stability than the polymer gel. The *in situ* SGC gel is a novel type of polymer gel developed in recent years.[39,40] With a combination of modified starch and monomers, this agent can form a three-dimensional (3D) crosslinked network-like macromolecular copolymer. As a result, the gel shows a high strength within the porous media for water plugging. Next, Song *et al.*[41] and Zhao *et al.*[42] introduced the use of SGC gel to treat fractures during the CO_2 flooding process. They revealed that the SGC gel has a stable plugging performance, which can improve oil recovery by more than 18% in the low permeability oil reservoirs.

The CO_2 and water resistance of the SGC gel, mentioned previously, make it possible to use it to assist with the CO_2 huff-n-puff process. However, the CO_2 huff-n-puff is a more temporary EOR method compared with CO_2 flooding, and furthermore, the edge-water invasion makes the plugging environment more complex. Therefore, it is necessary to study the EOR mechanisms of the gel assisted CO_2 huff-n-puff process. To enable the selection of the best process, the static and dynamic performances of polymer gel and SGC gel were also compared in this research. The viscosities and rheological performances of polymer gel and SGC gel are first evaluated in bulk experiments, then the injectivity and plugging ability are studied using one-dimensional (1D) sand packs. The 3D physical models with water channels are then established in the laboratory, and pure CO_2 huff-n-puff and gel assisted CO_2 huff-n-puff experiments are conducted after edge-water driving. Pilot tests of gel assisted CO_2 huff-n-puff are also discussed in this paper.

2. Experiments

2.1 Rheological evaluations of polymer gel and SGC gel

A polymer gelant and a SGC gelant with similar viscosities were prepared in the laboratory for use in the rheological evaluations. Formation water with a salinity of 1937 mg L^{-1} was used for the preparation, which was collected from the reservoir

block. For the polymer gelant preparation, 0.15 wt% of HPAM (molecular weight of 25 million Da), and 0.04 wt% of an inorganic crosslinker were mixed with the formation water. For the SGC gelant, 2.0 wt% of α-starch, 2.0 wt% of acrylamide (AM) monomer and 0.02 wt% of an organic crosslinker were mixed with the formation water. After the preparation, the viscosities of the polymer gelant and the SGC gelant were first measured using a Brookfield NDJ-1C viscometer with a shear rate of 7.31 s^{-1}. A temperature of 65 °C was set as the formation temperature.

Then, the rheological behaviors of the polymer gelant and the SGC gelant were evaluated using a HAAKE RS600 rheometer. The temperature was also set as 65 °C, and the angular frequency ranged from 0.1 rad s^{-1} to 1000 rad s^{-1}. The storage modulus G', loss modulus G'' and phase angle δ were obtained during the evaluation. G' can be used to evaluate the elastic property of the pseudoplastic fluid, and G'' can be used to evaluate the viscosity of the fluid.[43,44] Then, the complex modulus G^* can be defined as:

$$|G^*| = |(G')^2 + (G'')^2|^{1/2} \quad (1)$$

The proportion of G' and G'' within the complex modulus G^* can be calculated as:

$$E_{els} = \frac{|G'| \times \sin\delta}{|G^*|} \times 100\% \quad (2)$$

$$E_{vis} = \frac{|G''| \times \sin\delta}{|G^*|} \times 100\% \quad (3)$$

where E_{els} is the proportion of the elastic property, and E_{vis} is the proportion of viscous property. The phase angle δ can be calculated as follows:

$$\tan\delta = |G''|/|G'| \quad (4)$$

When the values of G' and G'' had been obtained, the values of E_{els} and E_{vis} were then determined to evaluate the elastic and viscous properties for the polymer gelant and the SGC gelant.

After the viscosity and rheology had been determined, the polymer gelant and the SGC gelant were placed in a container for 24 h for the gelation process to occur. The container was resistant to CO_2 corrosion, and could hold a high-temperature and high-pressure (HTHP) condition as shown in Fig. 1. The temperature was set at 65 °C, and the pressure was maintained as 15 MPa by CO_2 (with a purity of 99.99 mol%). After the gelation, the viscosities of the polymer gel and the SGC gel were again measured using the viscometer, and the G' and G'' values of the gels were also determined using the rheometer.

2.2 The 1D injectivity and plugging experiments of the polymer gel and the SGC gel

The injectivity and plugging performance of the polymer gel and the SGC gel were then studied using 1D sand packs. The sand packs with an average permeability of 8000 × 10^{-3} μm^2 were utilized to simulate the high permeable water channels, and the diameter of the sand pack was 25 mm, and was the length is 1000 mm, and the other physical parameters of the sand packs are listed in Table 1. The formation water and chemical agents used in the 1D experiments were the same as mentioned previously.

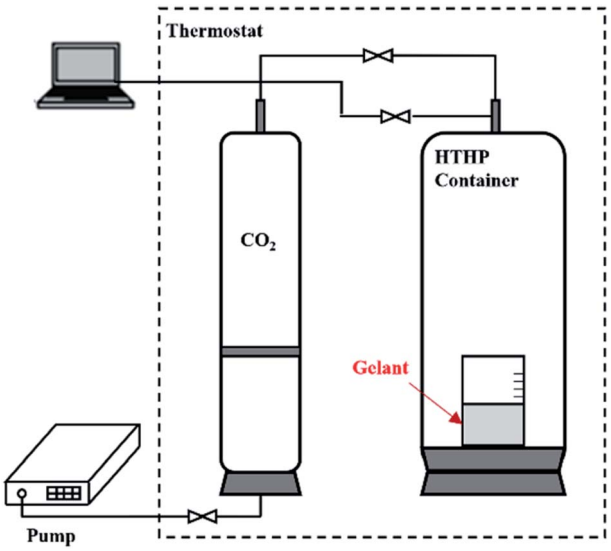

Fig. 1 Flow chart of the gelation process.

The core was firstly vacuumed and then saturated with formation water. The experimental temperature was set to 65 °C, and then a primary waterflooding process was conducted with a constant injection rate of 0.3 mL min^{-1}. When the waterflooding pressure reached a steady state, the gelant was injected until a certain volume was reached. After 24 h of gelation, another waterflooding process was again conducted with the same injection rate. When the volume of the second waterflooding water reached 2.0 PV, the experiment was terminated. During the experimental process, the primary waterflooding pressure (p_{wb}), the gelant injection pressure (p_{gel}), the water breakthrough pressure (p_{wB}) and the second waterflooding pressure (p_{wa}) can be obtained. Then, a resistance factor (RF) of gelant can be calculated using the waterflooding pressure (p_{wb}) and the gelant injection pressure (p_{gel}) as shown in eqn (5). Because the RF was related to the p_{gel}, it can be used to reflect the injectivity of the gelant:

Table 1 Physical parameters of 1D artificial cores

Gel type	Gelant injection volume/PV	Permeability/×10^{-3} μm^2	Porosity/%
Polymer gel	0.025	8208	40.75
	0.05	8461	41.54
	0.075	8737	42.63
	0.10	7463	37.99
	0.15	8260	41.06
SGC gel	0.01	7694	39.89
	0.02	8152	40.67
	0.03	7509	38.29
	0.05	7153	36.99
	0.075	8633	42.11
	0.10	7985	40.09

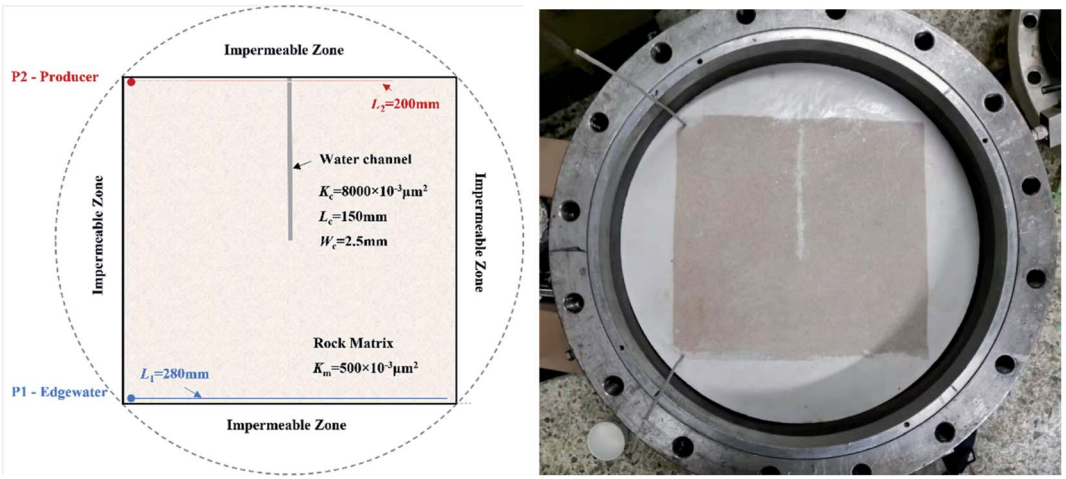

Fig. 2 A 3D physical model for SGC gel assisted CO_2 huff-n-puff. (a) Design of the 3D model (b) picture of a 3D model.

$$RF = \frac{K_{gel}/\mu_{gel}}{K_{wb}/\mu_w} = \frac{p_{gel} - p_0}{p_{wb} - p_0} \quad (5)$$

where K_{wb} is the permeability of the water before gelation, ($\times 10^{-3}$ μm^2), K_{gel} is the permeability of the gelant ($\times 10^{-3}$ μm^2), μ_w is the viscosity of the water phase (mPa s), μ_{gel} is the viscosity of the gelant, (mPa s), and p_0 is the outlet pressure of the core (kPa), which was set as standard atmospheric pressure during the experiment.

When the water breaks through the gel and maintains a steady state after 2.0 PV of injection, a residual resistance factor (RRF) can be calculated using the primary waterflooding pressure (p_{wb}) and the second waterflooding pressure (p_{wa}) as shown in eqn (6). Because the RRF was a comparison of water flow ability before and after gelation, it can be used to reflect the plugging performance of the gel:

$$RRF = \frac{K_{wa}/\mu_w}{K_{wb}/\mu_w} = \frac{p_{wa} - p_0}{p_{wb} - p_0} \quad (6)$$

where K_{wa} is the permeability of water after gelation ($\times 10^{-3}$ μm^2).

The injectivity and plugging performance of the polymer gel and the SGC gel were evaluated, and different injection volumes of the gelants were determined in the 1D sand packs. The injection volume ranged from 0.025 PV to 0.15 PV for the polymer gelant, and ranged from 0.01 PV to 0.10 PV for the SGC gelant. For each scenario, the experimental procedures were repeated as mentioned previously.

2.3 The 3D experiments for SGC gel assisted CO_2 huff-n-puff

The 3D physical models were designed in the laboratory to study the EOR mechanisms of the SGC gel assisted CO_2 huff-n-puff. The size of the model was 300 × 300 × 45 mm^3 with a matrix permeability (K_m) of 500 × 10^{-3} μm^2, and two horizontal wells were located on the opposite side of the model as shown in Fig. 2. Well P1 with a length of 280 mm was used for edge-water injection, and well P2 with a length of 200 mm was used as a producer. A water channel with a size of 150 × 25 × 45 mm^3 was created which was orthogonal to P2 in the 3D model, and the permeability of the channel (K_c) was 8000 × 10^{-3} μm^2. Four impermeable zones were fabricated beside the four sides of the model in order to fit the 3D core holder, and no fluids could be exchanged between the permeable and impermeable zones. The physical parameters of the 3D models are shown in Table 2. A 3D core holder was specially designed for the HTHP displacement experiments with an operational temperature of 0–120 °C and an operational pressure of 0–30 MPa (as shown in Fig. 2(b)). The formation water, CO_2 and chemical agents used in the 3D experiments were the same as mentioned previously. The formation oil was collected from the reservoir block. The density of the formation oil was 0.89 g cm^{-3}, the viscosity was 58.21 mPa s, and the gas/oil ratio was 42.42 m^3 m^{-3} under formation conditions (65 °C, 15 MPa).

Fig. 3 shows the flow chart for the 3D experiments using gel assisted CO_2 huff-n-puff. The experimental setup consisted of six sub-systems: an injection system, an edge-water injection

Table 2 The physical parameters of the 3D experimental models[a]

No.	Experimental scheme	Apparent volume/mL	Pore volume/mL	Porosity/%	Permeability/$\times 10^{-3}$ μm^2	Initial oil saturation/%
1	CO_2 huff-n-puff	4032	1054	26.14	K_m = 500	59.14
2	SGC gel assisted CO_2 huff-n-puff	4036	1047	25.94	K_c = 8000	58.76

[a] Where K_m is the permeability of the matrix ($\times 10^{-3}$ μm^2), and K_c is the permeability of the water channel $\times 10^{-3}$ μm^2).

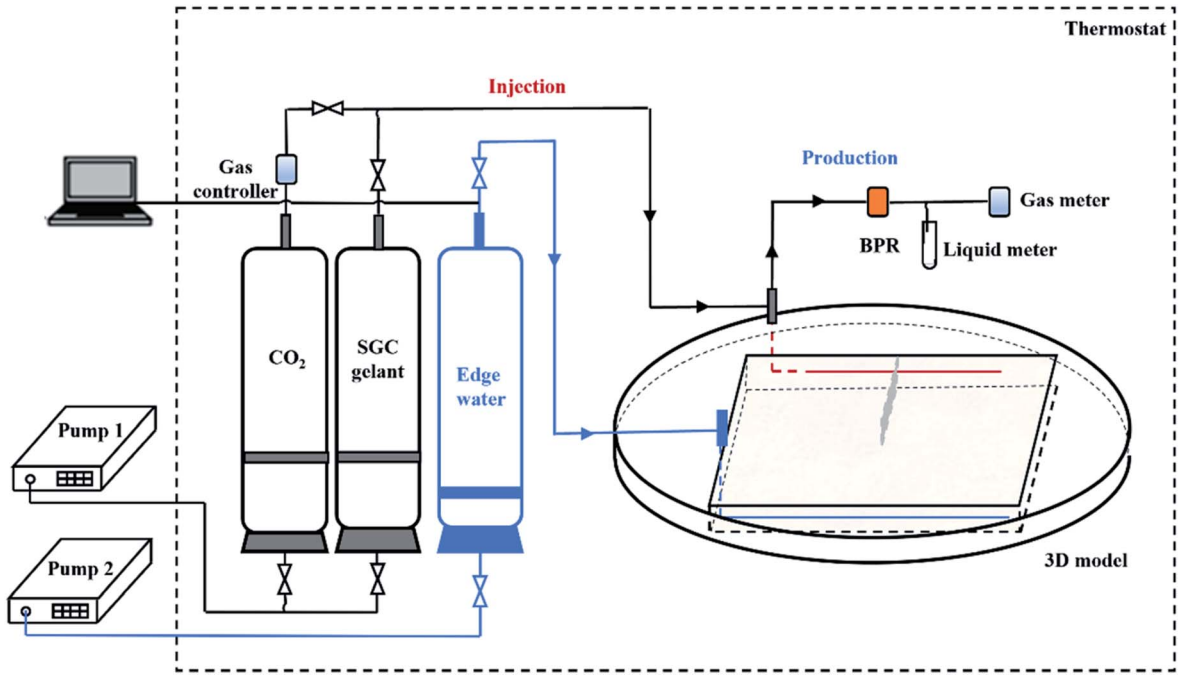

Fig. 3 Flow chart of the 3D experiments using gel assisted CO_2 huff-n-puff.

system, a displacement system, a production system, a temperature control system, and a data acquisition system. In the injection system, CO_2 and SGC gelant were stored in transfer cylinders and then injected into the model by a constant pressure and rate pump. In the edge-water injection system, formation water was stored in the cylinder and then injected into the model through P1. The 3D physical model was placed in the core holder with a confining pressure. In the production system, a backpressure regulator (BPR) was connected with P2 to control the production pressure. The produced oil and water were collected in test tubes and the volumes were measured, and the gas was measured using a gas flow meter. The thermostat was used to maintain the experimental temperature, and the displacement pressures of P1 and P2 were obtained by the data acquisition system. The physical parameters of the 3D models are listed in Table 2. An experiment using a pure CO_2 huff-n-puff system was also conducted for comparison.

Scenario 1 was utilized for the CO_2 huff-n-puff experiment, and the experimental procedure was as follows: (1) the 3D model was held by the core holder, and then placed into the thermostat at a temperature of 65 °C. The production pressure of P2 was set to 15 MPa to maintain the formation pressure. Then, the formation water and oil were injected into the model to form the initial oil and water saturation. (2) The water was injected through P1 with an injection rate of 0.5 mL min^{-1} to simulate edge-water driving. After the water cut of P2 reached 98%, the edge-water driving process was terminated. (3) The CO_2 was injected into the model through P2 until the pressure reaches 20 MPa. After 24 h of soaking time, P1 and P2 were reopened for production. When the water cut of P2 reached 98% again, one cycle of CO_2 huff-n-puff was completed. The injection of gas, the production of oil, water and gas, and the displacement pressure were recorded during the experimental process. (4) Three more cycles of CO_2 huff-n-puff processes were conducted using the 3D model, and the oil recovery of edge-water driving and CO_2 huff-n-puff were calculated after the experiment.

Scenario 2 was utilized for the SGC gel assisted CO_2 huff-n-puff experiment. The experimental processes of preparation and edge-water driving were the same as for Scenario 1, whereas the procedures of gel assisted CO_2 huff-n-puff were as follows: (1) firstly, P2 was opened as a production well to ensure that the gelant can be injected into the model, then 5 mL of SGC gelant was injected through P1. P1 and P2 were then closed for 24 h to allow the gelation process to occur. (2) The CO_2 was injected into the model through P1 until the pressure reached 20 MPa. P1 and P2 were then reopened for production after a soaking time of 24 h. When the water cut of P2 reached 98% again, one cycle of gel assisted CO_2 huff-n-puff was completed. (3) Three more cycles of gel assisted CO_2 huff-n-puff processes were conducted on the 3D model, and the oil recovery enhanced by SGC gel assisted CO_2 huff-n-puff was calculated after the experiment.

3. Results and discussion

3.1 Performance comparisons of SGC gel and polymer gel

3.1.1 Comparison of rheological performance. Firstly, the polymer gelant and starch graft copolymer (SGC) gelant with similar viscosities were compared in the laboratory. At the formation temperature of 65 °C, the viscosity of the polymer gelant was 39.60 mPa s at a shear rate of 7.31 s^{-1}, and the viscosity of the SGC gelant was 37.95 mPa s. Although these two gelants were both pseudoplastic fluids, their rheological

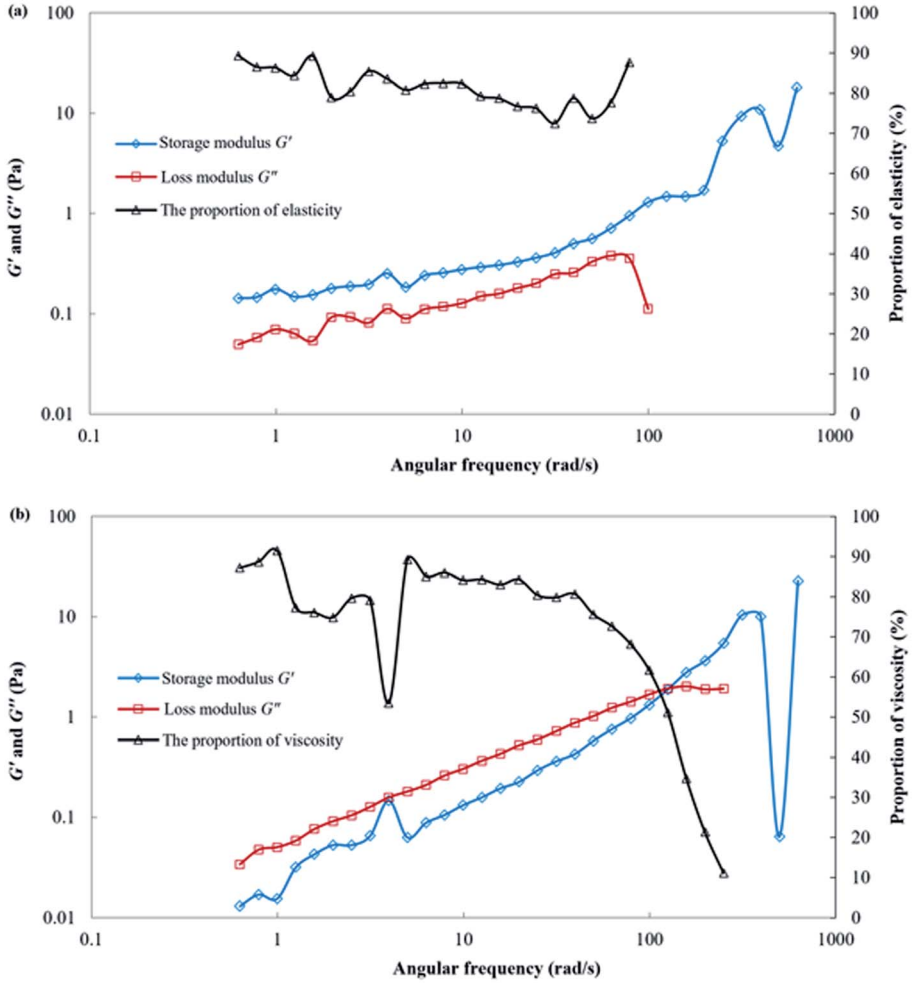

Fig. 4 Rheological performance of the gelants: (a) the polymer gelant and (b) the SGC gelant.

behaviors were quite different. Fig. 4(a) shows that the storage modulus G' is higher than the loss modulus G'' for the polymer gelant, which indicated that the elastic property of the gelant was stronger than its viscous property. The proportion of elastic property (E_{ela}) calculated from eqn (2) was within the range of 72.48% to 89.31%, meaning that the polymer gelant was predominantly an elastic solution. The elastic deformation and its recovery of molecular coils may cause injectivity problems in the porous media for the polymer gelant. However, the loss modulus G'' was higher than the storage modulus G' for the SGC gelant as shown in Fig. 4(b), which indicated that the viscous property of the gelant was stronger than its elastic property. The proportion of the viscous property (E_{vis}) was calculated to be more than 80% with an angular frequency of less than 40 rad s^{-1}, meaning that the SGC gelant was predominantly a viscous solution at the formation conditions used. The viscous property of the gelant can make it easier to flow through the pore throats, which may be favorable for its injectivity into the porous media.

After 24 h of gelation, both the polymer gelant and the SGC gelant can form solid-like gels. The viscosity of the polymer gel was 22 558 mPa s, whereas the viscosity of the SGC gel was as high as 174 267 mPa s. The rheological behaviors of the polymer gel and the SGC gel are shown in Fig. 5. For these two gels, the storage modulus G' was significantly higher than the loss modulus G'', and the proportion of the elastic property (E_{ela}) was more than 99% at low frequencies. As a result, both gels could form strong barriers for plugging within the porous media, and then force the successive water or gas to displace the upswept area for oil recovery. In addition, the G' and G'' of the SGC gel were also significantly higher than those of the polymer gel. The SGC gelant can form a higher strength gel when compared with that of the polymer gelant, which showed it had more potential for use in applications for channeling treatments during the CO_2 huff-n-puff process.

The microstructures of the polymer gel and the SGC gel were studied using SEM analysis, and the scanned images were compared and are shown in Fig. 6. For the polymer gel, the polymer chain was crosslinked with another chain, and then formed a continuous network structure.[40] The skeleton structure of the gel constructed by crosslinked the molecules can be clearly observed from Fig. 6(a). However, the structure of the SGC gel could not be seen properly until the gel was destroyed artificially. The gel surface was smooth and flat, but its interior showed a tighter crosslinked structure (as shown in Fig. 6(b)).

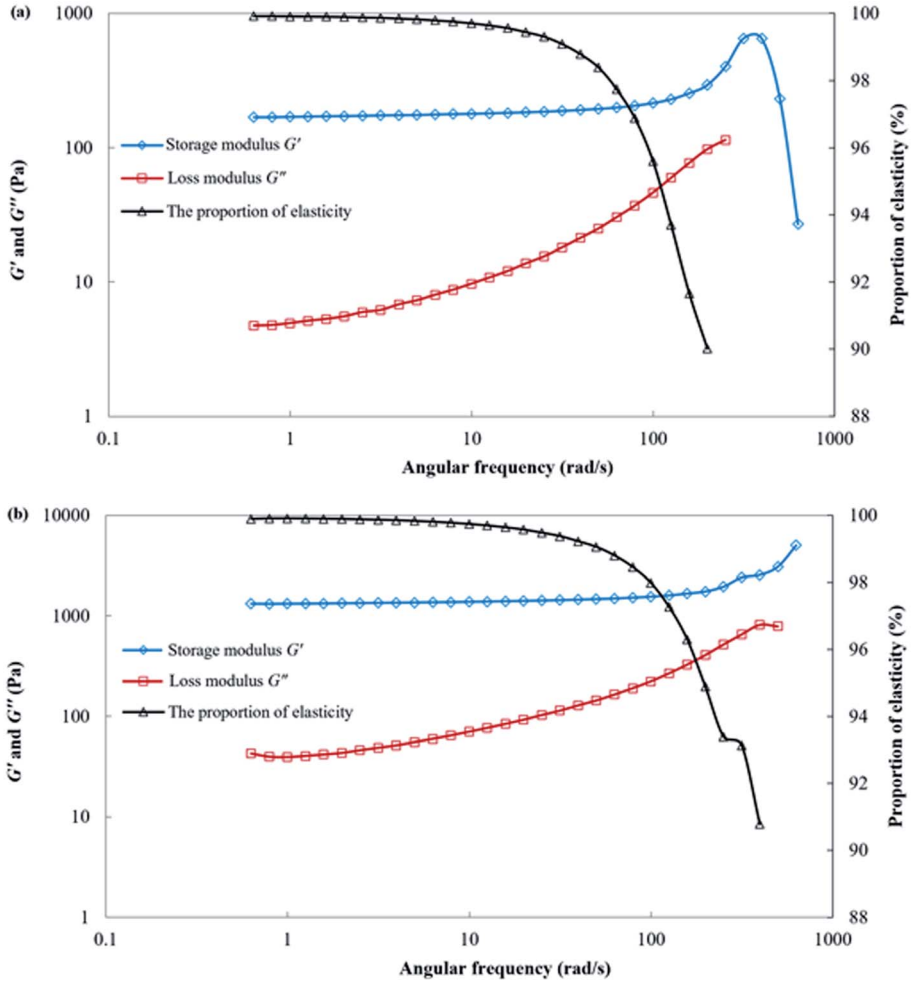

Fig. 5 Rheological performances of the gels: (a) polymer gel and (b) SGC gel.

The α-starch molecules can function as rigid skeletons, and then the skeletons can be flexibly filled with the AM.[45] After the crosslinking reactions, a more complex 3D network-like structure was formed, which had a higher strength when compared with the polymer gel.

3.1.2 Comparison of the injectivity and plugging performances. The injectivity and plugging performances of the SGC gel and the polymer gel were then compared using 1D sand packs, and the experimental results are shown in Table 3. Because the sand packs used to simulate the water channels

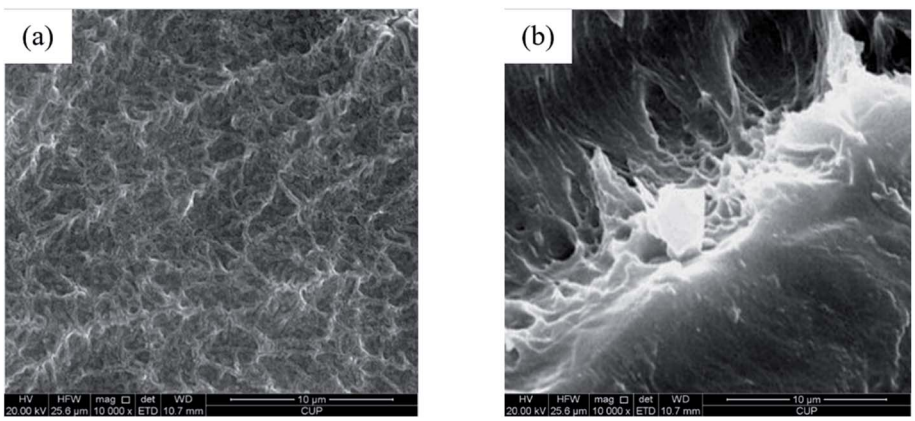

Fig. 6 The microstructures of the polymer gel and the SGC gel scanned by SEM: (a) polymer gel and (b) SGC gel. Magnified by 10 000 times.

Table 3 Pressure results of injectivity and plugging experiments in 1D artificial cores

Gel type	Gel injection volume/PV	Waterflooding pressure (p_{wb})/kPa	Gelant injection pressure (p_{gel})/kPa	Successive waterflooding	
				Breakthrough pressure (p_{wB})/kPa	Residual pressure (p_{wa})/kPa
Polymer gel	0.025	1.4	6.1	146.8	144.3
	0.05	1.4	10.1	202	179.7
	0.075	1.3	13.8	229.6	192.8
	0.10	1.6	23.1	322.2	243.8
	0.15	1.4	33.1	385.6	229.8
SGC gel	0.01	1.5	3.4	820.3	819.3
	0.02	1.5	4.1	857.5	847.8
	0.03	1.6	5.6	943	935.6
	0.05	1.7	6.8	1047.6	1000.7
	0.075	1.4	8.9	925.7	849.4
	0.10	1.5	12.7	997.1	923

had a high permeability of 8000 $\times$ 10^{-3} μm^2, the waterflooding pressures (p_{wb}) were lower than 1.7 kPa. Then, different volumes of gelants were injected after waterflooding. With the increase of the gelant injection volume, the injection pressure (p_{gel}) gradually increased for both the SGC gelant and the polymer gelant. It was observed that the injection pressure of the SGC gelant was less than that of the polymer gelant. Taking a volume of 0.10 PV as an example, the pressure of the SGC gelant was only 0.38 times higher than that of the polymer gelant. This means that the SGC gelant had a much better injectivity with the same injection volume when compared with that of the polymer gelant. After a gelation process of 24 h, the waterflooding was conducted for each scenario. When the water breaks through the gel, the waterflooding pressure increased from less than 1.7 kPa (p_{wb}) to hundreds of kPa (p_{wB}), which showed that both the polymer gel and the SGC gel effectively plugged the channels. After 2.0 PV of successive waterflooding, the residual pressure (p_{wa}) still remained at a value of hundreds of kPa, which means that both the polymer gel and the SGC gel had a good stability for plugging. Furthermore, both the breakthrough pressure (p_{wB}) and the residual pressure (p_{wa}) of the SGC gel were 3 to 5 times higher than those of the polymer gel, which meant that the SGC gel had a better plugging performance when compared with the polymer gel.

The different injectivity and plugging performances of the SGC gel and the polymer gel were determined using the resistance factors (RF) and the residual resistance factors (RRF). The resistance factor of the gelant retains an exponential growth with the injection volume for both the SGC gelant and the polymer gelant as shown in Fig. 7. From the fitting curves, an empirical formula can be obtained:

$$RF = a \exp(bV_{gel}) \quad (7)$$

where a and b are the coefficients, and V_{gel} is the gelant injection volume. For the polymer gelant, $a = 3.5496$, and $b = 13.272$, and for the SGC gelant, $a = 2.063$, and $b = 14.399$. The coefficient a of the SGC gelant was 0.58 times higher than that of the polymer gelant. Although the polymer gelant and the SGC gelant had similar viscosities in bulk conditions, the SGC gelant showed a better injectivity in porous media when compared with the polymer gelant. As mentioned previously, the polymer gelant was a predominantly elastic solution under low shear conditions. When the polymers were injected into the porous

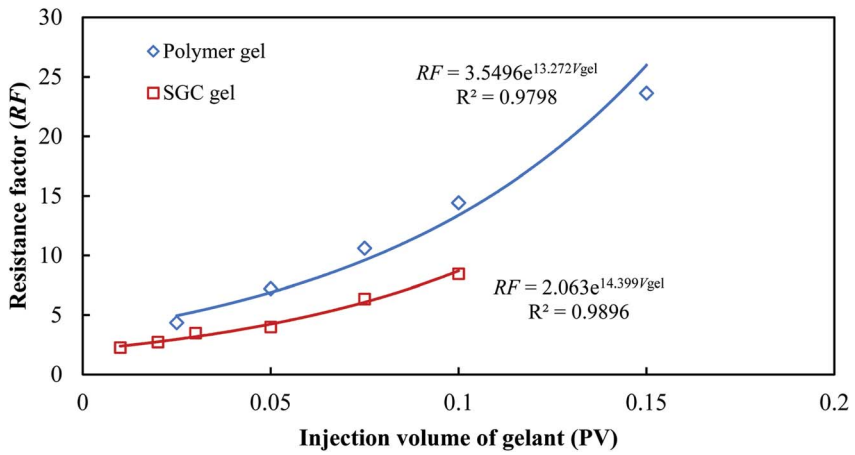

Fig. 7 Comparison of the resistance factors (RF) for the SGC gelant and the polymer gelant.

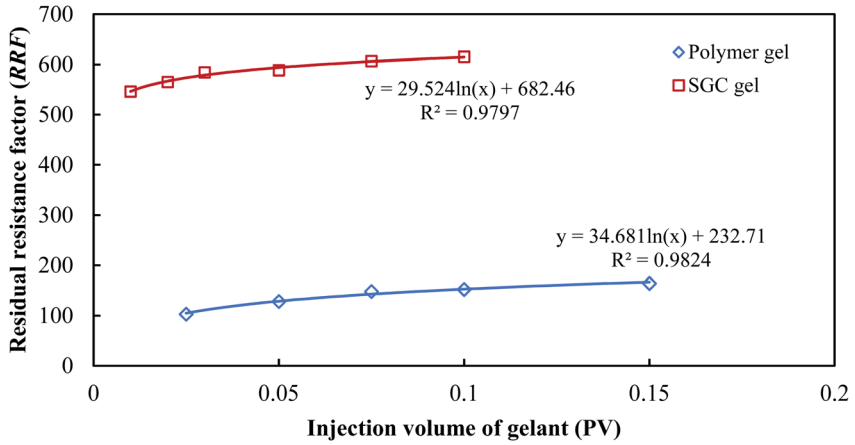

Fig. 8 Comparison of the residual resistance factors (RRF) for the SGC gel and the polymer gel.

media, the molecular coils deformed elastically according to the different sizes of the pore throats, which then caused a higher flow resistance for the polymer gelant. This result was also consistent with the idea proposed by Alfazazi *et al.*[46] that the polymers might have good rheology in bulk experiments but end up with poor injectivity in porous media, whereas the SGC

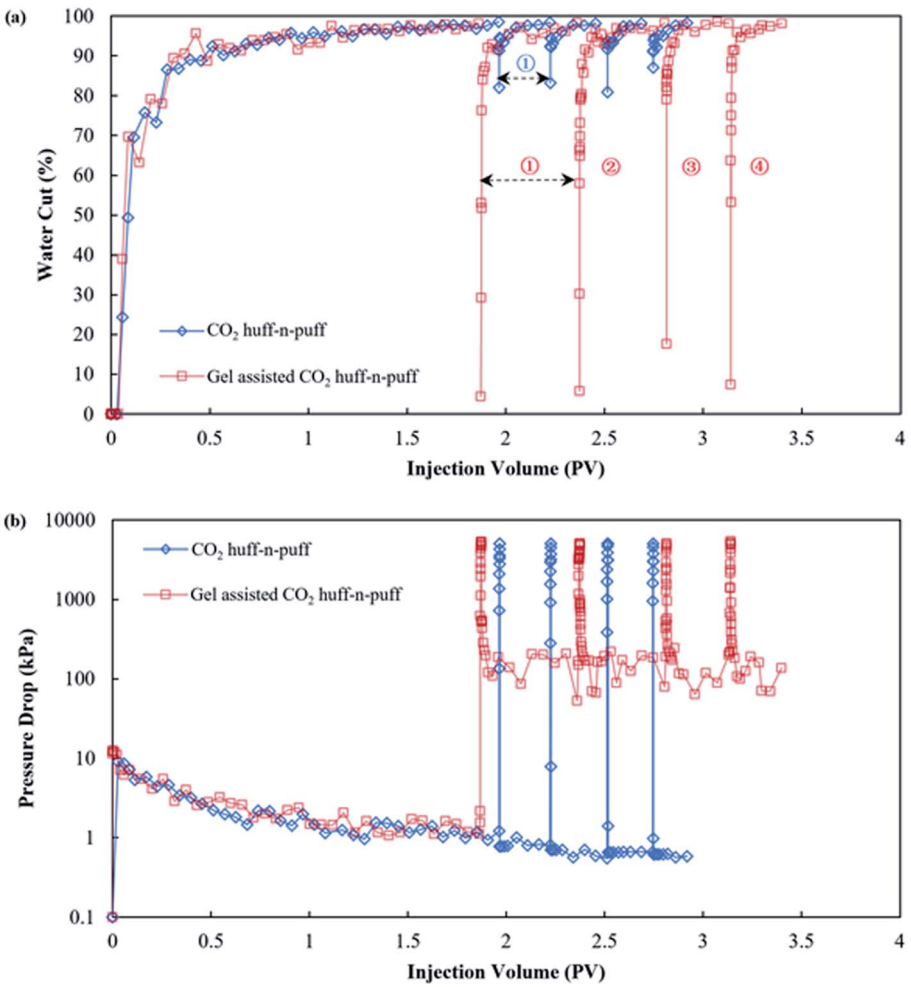

Fig. 9 Production performances of pure CO_2 huff-n-puff and gel assisted CO_2 huff-n-puff processes: (a) water cut comparison and (b) pressure drop comparison.

Table 4 The 3D experimental results of pure CO_2 huff-n-puff and gel assisted CO_2 huff-n-puff processes

No.	Period	Cycle no.	SGC gel volume/mL	CO_2 volume (surface)/mL	Production oil volume/mL	Oil recovery factor/%	Lowest water cut/%	Valid production time /PV
1	Edgewater driving	—	—	—	211.38	33.90	—	1.96
	CO_2 huff-n-puff	1st	—	1279	7.99	1.28	92.85	0.26
		2nd	—	1262	7.39	1.19	92.37	0.23
		3rd	—	1236	6.20	0.99	91.67	0.23
		4th	—	1244	6.09	0.98	91.23	0.23
	Total	—	—	5021	239.05	38.34	—	2.91
2	Edge water driving	—	—	—	196.15	31.88	—	1.87
	SGC gel assisted	1st	5	1262	23.95	3.89	4.41	0.50
	CO_2 huff-n-puff	2nd	5	1239	22.24	3.61	5.79	0.44
		3rd	5	1205	13.13	2.13	17.58	0.33
		4th	5	1234	10.63	1.73	7.37	0.26
	Total	—	20	4940	266.10	43.24	—	3.40

gelant was a predominantly viscous solution at low shear conditions. The molecular chains of starch could be easily arranged according to the size of pore throats, which then caused a lower flow resistance in the porous media.

The RRF retains a logarithmic growth with the injection volume for both the SGC gelant and the polymer gelant as shown in Fig. 8, which can also be fitted as:

$$\mathrm{RRF} = c \ln(V_{\mathrm{gel}}) + d \quad (8)$$

where c and d are the coefficients. For the polymer gelant, $c = 29.524$, and $d = 682.46$, and for the SGC gelant, $c = 34.68$, and $d = 232.71$. The coefficient d of the SGC gel was 2.93 times higher than that of the polymer gel, which means that the plugging ability of the SGC gel was about three times higher than that of the polymer gel. For example, the RRF value of the SGC gel with the lowest volume of 0.01 PV was 546, which was 3.33 times higher than that of the polymer gel with a volume of 0.15 PV. The 3D network-like structure of the SGC gel built a stronger barrier within the porous media,[47,48] and even a small volume of gel could achieve an excellent plugging performance, which was favorable for assisting the CO_2 huff-n-puff process. It was also observed that the RRF value gradually increased when the gelant volume was less than or equal to 0.03 PV, but it scarcely increased when the volume exceeded 0.03 PV. This shows that the 0.03 PV of the gelant was strong enough for the plugging treatment in high permeable channels.

3.2 The EOR mechanisms of the SGC gel assisted CO_2 huff-n-puff

In order to study the EOR mechanisms of the SGC gel assisted CO_2 huff-n-puff in a water channeling reservoir, 3D experiments were conducted in the laboratory and the results are shown in Table 4. A pure CO_2 huff-n-puff experiment was conducted after edge-water driving in Scenario 1 for a comparison. The oil recovery of the edge-water driving was 33.90% when the water cut of the producer reached 98%. Then, four cycles of CO_2 huff-n-puff processes were conducted with an average CO_2 volume of 1255 mL (surface conditions) for each cycle. However, the oil recovery factors were only 1.28%, 1.19%, 0.99% and 0.98% for the 1st, 2nd, 3rd and 4th cycles, respectively. Due to the existence of the water channels, the edge-water mostly flowed through the channel, leaving plenty of formation oil, and the injected CO_2 remained at the rock matrix. For the SGC gel assisted CO_2 huff-n-puff experiment in Scenario 2, a similar remaining oil saturation was found with an oil recovery of 31.88% after the edge-water driving. Then, the SGC gel with a volume of 5 mL (calculated as 0.03 PV of the water channels) was first injected into the core, followed by a similar CO_2 volume of 1239 mL for each cycle. After the channel was plugged, the oil recovery factor was enhanced to 3.89%, 3.61%, 2.13% and 1.73% for the 1st, 2nd, 3rd and 4th cycles, respectively. The total oil recovery enhanced by gel assisted CO_2 huff-n-puff was 11.36%, which was 2.56 times higher than that of the pure CO_2 huff-n-puff process. Fig. 9(a) compares the water cuts of the pure CO_2 huff-n-puff, and gel assisted CO_2 huff-n-puff

Table 5 Pilot test results of the gel assisted CO_2 huff-n-puff process

Well no.	Cycle	Operation period	Gel volume/m^3	CO_2 volume/m^3	Oil production/m^3	Lowest water cut/%	Valid production time/day
G104-5CP13	1st	2017.01–2017.11	320	21 551	508.70	46.8	221
	2nd	2018.03–2019.03	400	22 727	632.90	51.5	326
G104-5P8	1st	2020.02–2020.09	450	19 305	382.39	40.0	181
G104-5P42	1st	2016.08–2017.07	850	24 385	310.16	65.6	237
	2nd	2017.07–2018.03	800	21 444	241.71	65.0	188
G104-5P60	1st	2020.03–2021.05	500	25 134	780.20	39.6	401
G207-4	1st	2018.08–2020.05	650	24 118	934.80	10.4	320

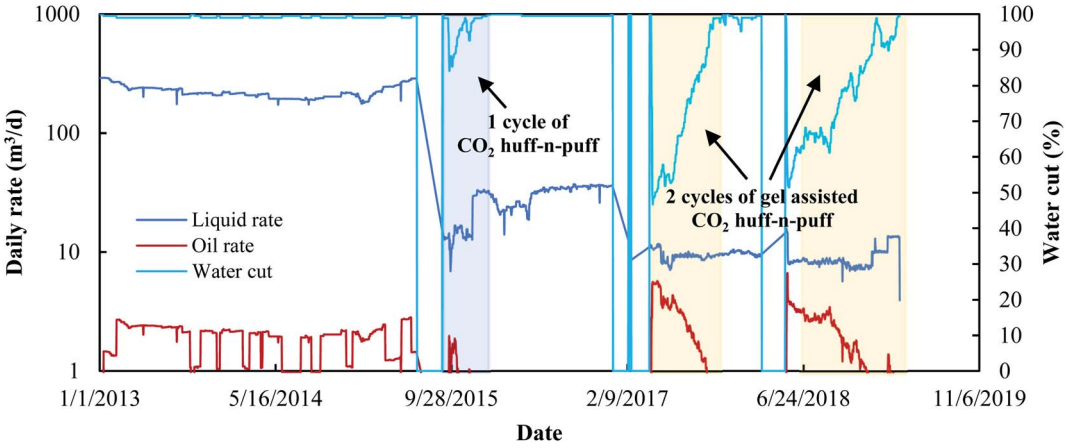

Fig. 10 Production performances of the G104-5CP13 oil well since 2013.

processes. For the pure CO_2 huff-n-puff experiment, the water cut firstly dropped to 91–93% at the initial production stage, and then increased sharply to about 96% when the edge-water broke through along the channel. After an average 0.24 PV of valid production time, the water cut reached 98% again. For the gel assisted CO_2 huff-n-puff experiment, the water cut dropped drastically to 4–18% at the initial stage, and an amount of crude oil was produced together with CO_2. Then, the water cut gradually increased to more than 90% with the driving of the edge water. The valid production time could also be greatly prolonged to 0.26–0.50 PV, which was about 1.6 times higher than that of the pure CO_2 huff-n-puff.

Fig. 9(b) compares the pressure drops of the pure CO_2 huff-n-puff and gel assisted CO_2 huff-n-puff. Similar pressure drops of about 1.5 kPa were observed during the edge-water driving periods for these two experiments, however, the drops show greater differences during the huff-n-puff period. For the pure CO_2 huff-n-puff experiment, the pressure drop decreased instantaneously from 5 MPa to less than 1 kPa at the initial stage of production. The edge-water broke through immediately along the channel, but the formation oil and injected CO_2 still remained within the rock matrix and could not be produced after water channeling. For the gel assisted CO_2 huff-n-puff experiment, the pressure drop gradually decreased from 5 MPa to about 500 kPa at the initial stage, where the oil was produced together with CO_2. Then, the pressure drop remained at a level of about 150 kPa until the end of the production stage, which was a hundred times greater than that of pure CO_2 huff-n-puff. After the successful plugging of the water channels using SGC gel, the remaining oil of the near-wellbore area was extracted by the injected CO_2 first, and the oil of the deep formation was then effectively displaced to the production well by the edge water, which showed that the injection of the gel enlarged the sweep efficiency of both CO_2 and the edge water.[49,50] The oil recovered from both the near-wellbore area and the deep formation showed that a remarkable oil enhancement had been achieved. The 3D experimental results showed that the SGC gel has great potential for assisting the CO_2 huff-n-puff for further enhanced oil recovery in the water channeling reservoir.

3.3 Pilot tests of the SGC gel assisted CO_2 huff-n-puff process

Several pilot tests of the SGC gel assisted CO_2 huff-n-puff process have been conducted in the North Gaoqian Block, Jidong Oilfield, China since 2016, and the results of five wells are shown in Table 5. Before the gel assisted CO_2 huff-n-puff operations, all the wells were facing severe water channeling problems with water cuts of more than 99%. Then, 320–850 m^3 of the gels were firstly injected into the wells for water channeling treatments, followed by CO_2 injection with an average volume of 22 666 m^3. After the wells were reopened for production, remarkable water control effects were obtained with the water cuts reaching as low as 10.4–65.6%. The valid production time of gel assisted CO_2 huff-n-puff ranged from 181 d to 401 d, and an average oil production of 542 m^3 was recovered by the gel assisted CO_2 huff-n-puff process during each cycle.

It was found that two cycles of the gel assisted CO_2 huff-n-puff process had been operated in the G104-5CP13 and G104-5P42 oil wells between 2017 and 2019. Taking G104-5CP13 as an example, its production performance since 2013 is shown in Fig. 10. This well faced the water channeling problem for more than five years with the water cut as high as 99%. One cycle of the huff-n-puff process with a CO_2 volume of 19 251 m^3 was conducted between 2015.07 and 2015.12, however, only 73.54 m^3 of oil was recovered by pure CO_2, and the water cut dropped to 85.5% and then increased rapidly to 99% again within 113 d. However, for the gel assisted CO_2 huff-n-puff, the water cut could drop to as low as 46.8%, and the valid production time could be prolonged to more than 200 d, and more than 500 m^3 of crude oil was recovered in the following two cycles. In addition, the oil rate could also be enhanced to more than 5.5 m^3 per day at the initial stage of the gel assisted CO_2 huff-n-puff, which was more than 3.5 times higher than those of edge-water driving and the pure CO_2 huff-n-puff process.

A total gel volume of 3970 m^3 was used for water channeling treatments in these eight wells, and the cumulative CO_2 volume

reached 15.87×10^4 m^3. A cumulative oil production of 3790.86 m^3 was obtained by the end of 2020, which showed that the gel assisted CO_2 huff-n-puff had economic benefits in the water channeling reservoir.

4. Conclusions

Gel assisted CO_2 huff-n-puff can be used for further enhanced oil recovery in a water channeling reservoir. The starch graft copolymer (SGC) gel is selected for the assisted process due to its better performances after a comparison with the polymer gel. Then, laboratory experiments and pilot tests of the SGC gel assisted CO_2 huff-n-puff were conducted to enhance oil recovery, and some of the conclusions obtained are summarized as follows:

(1) Although the bulk viscosities of the polymer gelant and the SGC gelant were similar, their rheological performances are quite different. The polymer gelant is a predominantly elastic solution, whereas the SGC gelant is a predominantly viscous solution, which makes it easier to inject it into the pore throats. The RF value of the SGC gelant is only 0.58 times greater than that of the polymer gelant, which shows that the SGC gelant has a better injectivity when compared with the polymer gelant.

(2) Both the polymer gelant and the SGC gelant can form solid-like gels, however, the strength of the SGC gel is much higher, with a viscosity of 174 267 mPa s. The results of the SEM analysis revealed that a more complex 3D network-like structure was formed using SGC gelant, and the RRF value of the SGC gel was about three times higher than that of the polymer gel. The higher strength of the SGC gel guarantees that a stronger barrier is formed within the high permeable water channels.

(3) The SGC gel assisted CO_2 huff-n-puff and pure CO_2 huff-n-puff are compared using 3D experiments, and the results show that four cycles of gel assisted CO_2 huff-n-puff achieve an oil recovery enhancement of 11.36%, which is 2.56 times greater than that using pure CO_2 huff-n-puff. For the gel assisted CO_2 huff-n-puff process, the water cut can drop to as low as 4–18%, the pressure drop gradually decreases and then remains at a level of about 150 kPa, and the valid production time can be prolonged to about 1.6 times greater than that of the pure CO_2 huff-n-puff process.

(4) After the channel is plugged by the SGC gel, the remaining oil of the near-wellbore area can be first extracted by CO_2, and the oil of the deep formation can then be effectively displaced by the edge water. With the combination of CO_2 extraction and edge-water driving, the oil remaining in rock matrix can be remarkably improved using the gel assisted CO_2 huff-n-puff process.

(5) Several pilot tests of the gel assisted CO_2 huff-n-puff process have been conducted in the North Gaoqian Block, Jidong Oilfield, China since 2016. With a total gel volume of 3970 m^3 assisted with 15.87×10^4 m^3 of CO_2 used in five wells, a cumulative oil production of 3790.86 m^3 was obtained by the end of 2020. From the pilot tests, it was found that gel assisted CO_2 huff-n-puff gave economic benefits, which can provide guidance for further enhanced oil recovery in similar oil reservoirs.

Conflicts of interest

The authors declare that there are no competing interests regarding the publication of this article.

Acknowledgements

This project is supported by the National Natural Science Foundation of China (Grant No. 52174046). The authors wish to acknowledge all their colleagues from Changzhou University, China University of Petroleum (Beijing), Exploration and Development Research Institute, PetroChina Daqing Oilfield Company, and the Drilling and Production Technology Research Institute of the PetroChina Jidong Oilfield Company, who all helped with this research.

References

1 S. Xu, Q. Feng, F. Guo, A. Yan, S. Liu, Y. Tao and X. Chen. Efficient development method for high-viscosity, complex Fault-block reservoir. *SPE Trinidad and Tobago Section Energy Resources Conference*, Port of Spain, Trinidad and Tobago, 2016.

2 Q. Yu, Z. Mu, P. Liu, X. Hu and Y. Li, A new evaluation method for determining reservoir parameters for the development of edge-water-driven oil reservoirs, *J. Pet. Sci. Eng.*, 2019, **175**, 255–265.

3 Z. Pang, Y. Jiang, B. Wang, G. Cheng and X. Yu, Experiments and analysis on development methods for horizontal well cyclic steam stimulation in heavy oil reservoir with edge water, *J. Pet. Sci. Eng.*, 2020, **188**, 106948.

4 Q. Feng, S. Li, Y. Su, Y. Liu and X. Han. Analyzing edge water drive laws of offshore heavy oil reservoir with physical experiment and numerical simulation. *SPE Energy Resources Conference*, Port of Spain, Trinidad and Tobago, 2014.

5 R. Cui, Q. Feng, Z. Li, F. Guo, A. Yan, S. Liu, Y. Tao and X. Chen. Improved oil recovery for the complex fault-block and multilayered reservoir with edge water. *SPE Trinidad and Tobago Section Energy Resources Conference*, Port of Spain, Trinidad and Tobago, 2016.

6 S. Seyyedsar, S. Farzaneh and M. Sohrabi, Experimental investigation of tertiary CO_2 injection for enhanced heavy oil recovery, *J. Nat. Gas Sci. Eng.*, 2016, **34**, 1205–1214.

7 A. Ahadi and F. Torrabi, Effect of light hydrocarbon solvents on the performance of CO_2-based cyclic solvent injection (CSI) in heavy oil systems, *J. Pet. Sci. Eng.*, 2018, **163**, 526–537.

8 A. Lobanov, K. Shhekoldin, I. Struchkov, M. Zvonkov, M. Hlan, E. Pustova, V. Kovalenko and A. Zolotukhin, Swelling/extraction test of Russian reservoir heavy oil by liquid carbon dioxide, *Petrol. Explor. Dev.*, 2018, **45**(5), 918–926.

9 X. Zhou, X. Li, D. Shen, L. Shi and Q. Jiang, CO_2 huff-n-puff process to enhance heavy oil recovery and CO_2 storage: An integration study, *Energy*, 2022, **239**, 122003.

10 C. Tian, Z. Pang, D. Liu, X. Wang, Q. Hong, J. Chen, Y. Zhang and H. Wang, Micro-action mechanism and macro-

prediction analysis in the process of CO_2 huff-n-puff in ultra-heavy oil reservoirs, *J. Pet. Sci. Eng.*, 2022, **211**, 110171.

11 S. Talebian, R. Masoudi, I. Tan and P. Zitha, Foam assisted CO_2-EOR: A review of concept, challenges, and future prospects, *J. Pet. Sci. Eng.*, 2014, **120**, 202–215.

12 B. Iraji, S. Shadizadeh and M. Riazi, Experimental investigation of CO_2 huff and puff in a matrix-fracture system, *Fuel*, 2015, **158**, 105–112.

13 J. Tetteh and R. Barati. Wettability alteration and enhanced oil recovery using low salinity waterflooding in limestone rocks: A mechanistic study. *SPE Kingdom of Saudi Arabia Annual Technical Symposium and Exhibition*, Dammam, Saudi Arabia, 2018.

14 A. Katende and F. Sagala, A critical review of low salinity water flooding: Mechanism, laboratory and field application, *J. Mol. Liq.*, 2019, **278**, 627–649.

15 J. Song, Q. Wang, I. Shaik, M. Puerto and G. Hirasaki, Effect of salinity, Mg^{2+} and SO_4^{2-} on ''smart water''-induced carbonate wettability alteration in a model oil system, *J. Colloid Interface Sci.*, 2020, **563**, 145–155.

16 J. Sheng, A comprehensive review of alkaline-surfactant-polymer (ASP) flooding, *Asia-Pac. J. Chem. Eng.*, 2014, **9**, 471–489.

17 R. Pogaku, N. Fuat, S. Sakar, Z. Cha, N. Musa, D. Tajudin and L. Morris, Polymer flooding and its combinations with other chemical injection methods in enhanced oil recovery, *Polym. Bull.*, 2018, **75**(4), 1753–1774.

18 L. Hedraningrat and O. Torsæter, Metal oxide-based nanoparticles: revealing their potential to enhance oil recovery in different wettability systems, *Appl. Nanosci.*, 2015, **5**, 181–199.

19 Y. Kazemzadeh, M. Sharifi, M. Riazi, H. Rezvani and M. Tabaei, Potential effects of metal oxide/SiO_2 nanocomposites in EOR processes at different pressures, *Colloids Surf., A*, 2018, **559**, 372–384.

20 M. Qu, T. Liang, J. Hou, Z. Liu, E. Yang and X. Liu, Laboratory study and field application of amphiphilic molybdenum disulfide nanosheets for enhanced oil recovery, *J. Pet. Sci. Eng.*, 2022, **208**, 109695.

21 M. Qu, T. Liang, L. Xiao, J. Hou, P. Qi, Y. Zhao, C. Song and J. Li, Mechanism study of spontaneous imbibition with lower-phase nano-emulsion in tight reservoirs, *J. Pet. Sci. Eng.*, 2022, **211**, 110220.

22 N. Anuar, M. Yunan, F. Sagala and A. Katende, The effect of WAG ratio and oil density on oil recovery by immiscible water alternating gas flooding, *American Journal of Science and Technology*, 2017, **4**(5), 80–90.

23 L. Wang, Y. He, Q. Wang, M. Liu and X. Jin, Multiphase flow characteristics and EOR mechanism of immiscible CO_2 water-alternating-gas injection after continuous CO_2 injection: A micro-scale visual investigation, *Fuel*, 2020, **282**, 118689.

24 K. Jessen, G. Tang and A. Kovscek, Laboratory and simulation investigation of enhanced coalbed methane recovery by gas injection, *Transp. Porous Media*, 2008, **73**, 141–159.

25 H. Hao, J. Hou, F. Zhao, H. Huang and P. Wang, Laboratory investigation of cyclic gas injection using CO_2/N_2 mixture to enhance heavy oil recovery in a pressure-depleted reservoir, *Arabian J. Geosci.*, 2020, **13**, 140.

26 F. Torabi, A. Kavousi, F. Qazvini and C. Chan, The feasibility of lab-scale cyclic CO_2 injection in fractured porous media, *Liq. Fuels Technol.*, 2014, **32**(7), 797–803.

27 K. Zhang, S. Li and L. Liu, Optimized foam-assisted CO_2 enhanced oil recovery technology in tight oil reservoirs, *Fuel*, 2020, **267**, 117099.

28 J. Solbakken and M. Aarra, CO_2 mobility control improvement using N_2-foam at high pressure and high temperature conditions, *Int. J. Greenh. Gas Control*, 2021, **109**, 103392.

29 R. Sydansk. A new conformance-improvement-treatment chromium(III) gel technology. *SPE enhanced oil recovery symposium*. Tulsa, Oklahoma, USA, 1988.

30 B. Sengupta, V. Sharma and G. Udayabhanu, Gelation studies of an organically crosslinked polyacrylamide water shut-off gel system at different temperatures and pH, *J. Pet. Sci. Eng.*, 2012, **81**, 145–150.

31 G. Zhao, C. Dai, A. Chen, Z. Yan and M. Zhao, Experimental study and application of gels formed by nonionic polyacrylamide and phenolic resin for in-depth profile control, *J. Pet. Sci. Eng.*, 2015, **135**, 552–560.

32 C. Zareie, A. Bahramian, M. Sefti and M. Salehi, Network-gel strength relationship and performance improvement of polyacrylamide hydrogel using nano-silica; with regards to application in oil wells conditions, *J. Mol. Liq.*, 2019, **278**, 512–520.

33 S. Asadizadeh, S. Ayatollahi and B. ZareNezhad, Fabrication of a highly efficient new nanocomposite polymer gel for controlling the excess water production in petroleum reservoirs and increasing the performance of enhanced oil recovery processes, *Chin. J. Chem. Eng.*, 2021, **32**, 385–392.

34 X. Sun, B. Bai, Y. Long and Z. Wang, A comprehensive review of hydrogel performance under CO_2 conditions for conformance control, *J. Pet. Sci. Eng.*, 2020, **185**, 106662.

35 F. Jin, L. Yang, X. Li, S. Song and D. Du, Migration and plugging characteristics of polymer microsphere and EOR potential in produced-water reinjection of offshore heavy oil reservoirs, *Chem. Eng. Res. Des.*, 2021, **172**, 291–301.

36 D. Bal, S. Patra and S. Ganguly, Effectiveness of foam-gel formulation in homogenizing the CO_2 front during subsurface sequestration, *J. Nat. Gas Sci. Eng.*, 2015, **27**, 994–1004.

37 Y. Zhang, M. Gao, Q. You, H. Fan, W. Li, Y. Liu, J. Fang, G. Zhao, Z. Jin and C. Dai, Smart mobility control agent for enhanced oil recovery during CO2 flooding in ultra-low permeability reservoirs, *Fuel*, 2019, **241**, 442–450.

38 B. Zhou, W. Kang, H. Yang, Z. Li and B. Sarsenbekuly, The shear stability mechanism of cyclodextrin polymer and amphiphilic polymer inclusion gels, *J. Mol. Liq.*, 2021, **328**, 115399.

39 R. Singh and V. Mahto, Synthesis, characterization and evaluation of polyacrylamide graft starch/clay

nanocomposite hydrogel system for enhanced oil recovery, *Petrol. Sci.*, 2017, **14**(4), 765–779.

40 D. Zhu, B. Bai and J. Hou, Polymer gel systems for water management in high temperature petroleum reservoirs: a chemical review, *Energy Fuels*, 2017, **31**(12), 13063–13087.

41 Z. Song, J. Hou, X. Liu, Q. Wei, H. Hao and L. Zhang, Conformance control for CO_2-EOR in naturally fractured low permeability oil reservoirs, *J. Pet. Sci. Eng.*, 2018, **166**, 225–234.

42 F. Zhao, P. Wang, S. Huang, H. Hao and G. Lu, Performance and applicable limits of multi-stage gas channeling control system for CO_2 flooding in ultra-low permeability reservoirs, *J. Pet. Sci. Eng.*, 2020, **192**, 107336.

43 H. Hao, J. Hou, F. Zhao, Z. Song, L. Hou and Z. Wang, Gas channeling control during CO_2 immiscible flooding in 3D radial flow model with complex fractures and heterogeneity, *J. Pet. Sci. Eng.*, 2016, **146**, 890–901.

44 H. Jia, H. Chen and J. Zhao, Development of a highly elastic composite gel through novel intercalated crosslinking method for wellbore temporary plugging in high-temperature reservoirs, *SPE J.*, 2020, **25**(6), 2853–2866.

45 Q. Luo, K. Tang, L. Bai, K. Li, P. Sun, C. Xu, Y. Zhao and D. Zhu, Development of in-situ starch grafted copolymerized gels for conglomerate reservoir conformance control and oil recovery improvement, *J. Pet. Sci. Eng.*, 2022, **210**, 110005.

46 U. Alfazazi, N. Thomas, W. Alameri and E. Al-Shalabi, Experimental investigation of polymer injectivity and retention under harsh carbonate reservoir conditions, *J. Pet. Sci. Eng.*, 2020, **192**, 107262.

47 J. Liu, L. Zhong, C. Wang, S. Li, X. Yuan, Y. Liu, X. Meng, J. Zou and Q. Wang, Investigation of a high temperature gel system for application in saline oil and gas reservoirs for profile modification. Journal of Petroleum Science and Engineering, *J. Pet. Sci. Eng.*, 2020, **195**, 107852.

48 S. Zhang, B. Peng and D. Luo, Formula optimization of thermosensitive biological sol–gel carrier for EOR surfactants by rheological investigation, *J. Pet. Sci. Eng.*, 2021, **205**, 108740.

49 S. Kumar and A. Mandal, A comprehensive review on chemically enhanced water alternating gas/CO_2 (CEWAG) injection for enhanced oil recovery, *J. Pet. Sci. Eng.*, 2017, **157**, 696–715.

50 P. Guo, Z. Tian, R. Zhou, F. Chen, J. Du, Z. Wang and S. Hu, Chemical water shutoff agents and their plugging mechanism for gas reservoirs: A review and prospects, *J. Nat. Gas Sci. Eng.*, 2022, **104**, 104658.